Korean J. Chem. Eng., 33(3), 1047-1058 (2016)
DOI: 10.1007/s11814-015-0163-2

pISSN: 0256-1115
eISSN: 1975-7220

Chemical potential and solid-solid equilibrium of near-spherical Lennard-Jones dumbbell crystal

Sangwon Lee, Minkyu Kim, and Jaeeon Chang†

Department of Chemical Engineering, University of Seoul, Siripdae-gil 13, Dongdaemun-gu, Seoul 130-743, Korea
(*Received 16 June 2015 • accepted 26 July 2015*)

Abstract−We studied the orientational order-disorder transition of crystals made up of near-spherical Lennard-Jones dumbbells, of which reduced bond lengths are 0.225, 0.250 and 0.275. Various techniques of Monte Carlo (MC) simulations are used to calculate the chemical potentials of ordered and disordered crystals, and thereby to predict order-disorder phase transition. First, we performed *NPT* MC simulations to determine crystal structure, equilibrium positions and orientations of the molecules. We then calculated the free energies of the crystals using the expanded ensemble MC simulations combined with the Einstein-molecule method and the thermodynamic integration method. The solid-solid phase equilibrium is determined from the free energy profiles of the individual phases by equating the chemical potential. The predictions of phase transition obtained from the conventional *NPT* MC simulation and the free energy simulation were in excellent agreement with each other, which confirms the validity of the present method of calculating the chemical potential of crystal. In addition, the Gibbs-Duhem integration was performed to obtain a complete coexistence curve between the two crystal phases. Orientational probability distributions of molecular axes were analyzed to find the characteristic behavior of rotational motion of molecule in the crystal. At sufficiently low temperature, flipping rotation of molecule in the ordered crystal is suppressed. In contrast, the flipping rotation occurs at higher temperature close to the transition while orientationally ordered structure is still maintained. In the free-energy calculation, such a unique rotational behavior requires to use a suitable form of external rotational potential with proper symmetry number. The present study demonstrates how one can judiciously choose a correct simulation scheme for the calculation of chemical potentials of molecular crystals.

Keywords: Free Energy, Entropy, Crystal, Lennard-Jones, Symmetry Number

INTRODUCTION

An important application of statistical thermodynamics to solid phase is to determine the most stable crystal structure from the knowledge of intermolecular interactions among constituting molecules. Even for simple molecules like nitrogen and carbon dioxide, there exist a variety of crystal structures depending on temperature and pressure of the system. Among many possible crystal structures, a structure with the lowest chemical potential is realized at equilibrium, and the collection of such knowledge on the entire range of temperature and pressure is represented as phase diagram. Therefore, the calculation of the chemical potential or free energy is important to understand the thermodynamic behavior of crystal system and plays a key role in predicting coexistence condition for multiple phases.

For solid phase, the Einstein-crystal method developed by Frenkel and Ladd has been widely used [1,2], in which the classical Einstein crystal of known free energy is used as a reference system. The difference in the free energy between the reference and real crystals is calculated by molecular simulations on a reversible path characterized by a coupling parameter that bridges the reference and real crystals. Recently, Vega and Noya [3] proposed a variant of the Einstein-crystal methods, the so-called Einstein-molecule method. Both methods are theoretically equivalent, and they give the same value of the free energy within simulation uncertainty. In practice, the Einstein-molecule method is easier to implement in molecular simulations.

Most molecular crystals made up of small and non-spherical molecules exist as orientationally ordered crystals in which the rotational motion of the molecule is restricted due to high energy barriers formed by its surrounding neighbors. This is in contrast to the molecules in fluid phases in which they can assume any orientations. The orientationally ordered crystal is non-ergodic in the sense that only a fragment of orientational configuration space is accessed in time by the evolution of physical process of the system. There are other type of molecular crystals called orientationally disordered crystals, i.e., plastic crystals in which molecule can rotate within its lattice cell. The molecules forming plastic crystals usually have near-spherical shapes such as methane, hexafluoroethane, SF_6, C_{60} and C_{70} fullerene molecules.

The entropy or free energy of molecular crystal should account for the orientational degeneracy or symmetry number of molecule [4,5]. The symmetry number plays the role of making quantum mechanical correction so as not to overcount indistinguishable orientational configurations. Whereas the symmetry number of a molecule in gas or liquid phase is considered to be constant, the symmetry number of the molecule in crystal depends on the extent of packing given by surrounding neighbor molecules. In orienta-

†To whom correspondence should be addressed.
E-mail: changjaee@uos.ac.kr

tionally disordered crystal, all the possible (but quantum mechanically identical) orientational configurations are realized by physical process, and the symmetry number is thus the same as that in the fluid phases. For example, the symmetry number for high-temperature C_{60} fullerene crystal is sixty [4], and for the phase I (plastic crystal) of methane is twelve [6]. However, in orientationally ordered crystal, only a single orientational state is realized out of the many possible orientational states. For this reason, a proper value of the symmetry number in the ordered crystal should be unity. It is understood that the symmetry number depends upon not only the inherent property of a molecule, but also the rotational characteristics of the molecule in condensed phase [5].

However, there are a few exceptional cases for which it is difficult to have a unique value of symmetry number. In certain crystals, some molecules can rotate in their lattice cells while the others are rotationally confined. In this case, it is necessary to assign different symmetry number for each molecule in the unit cell. Another problematic situation is related to orientational order-disorder transition. Far below transition temperature, the ordered crystal system samples only a fragment of the orientational configuration space, which is consistent with the symmetry number of unity. As temperature becomes close to the transition temperature, some molecules propelled with larger kinetic energy may cross over the rotational barrier. The rotational barrier-crossing, which has been referred to as orientational defect in the ordered crystal [4], actually occurs in real systems. However, in the aspect of calculating entropy and free energy it would be difficult to deal with such a sudden expansion of the accessible region in the configuration space triggered by the barrier-crossing. Thus, it is necessary to understand how we can relate the symmetry number to the rotational characteristics of molecules in crystal and also to the functional form of external rotational potential used in free energy calculations.

The main goal of the present work is to address how one can cope with the aforementioned rotational barrier crossing occurred in ordered crystal when calculating the free energy of the crystal close to order-disorder transition. As a simple model, we consider homonuclear Lennard-Jones dumbbell (LJ-d) of short bond length. This near-spherical LJ diatomic model forms orientationally ordered crystal at low temperature, while it forms orientationally disordered crystal at high temperature prior to melting. Because of the small anisotropy of the LJ-d model, the order-disorder transition may be observed in conventional molecular simulations by varying the temperature and pressure. Another advantage is that by using a well-defined theoretical model any ambiguity in the intermolecular interactions can be avoided. A closely related model is hard-sphere dumbbell model, for which many simulation studies have been done on the orientational order-disorder transition. Singer and Mumaugh [7] first predicted plastic crystal-fluid coexistence of fused hard dumbbells of the reduced bond length $L^*(=L/\sigma)<0.4$ where L is the bond length and σ is the size of segment. Monson and his coworkers extensively studied the solid-fluid equilibria of the hard dumbbells [8-10]. They predicted athermal order-disorder transitions among the ordered crystals of CP1, CP2 and CP3 structures and disordered (plastic) crystal of FCC structure. It was found that the disordered crystal phase of the hard dumbbells becomes stable at low pressure when $L^*<0.38$, and that among the ordered crystals the CP1 structure, in which dumbbell molecules are arranged in an ABC sequence similar to the FCC structure, is the most stable phase at high pressure. Later, Vega et al. predicted the phase diagram of tangential LJ diatomic model of $L^*=1$ for fluid-solid equilibrium and vapor-liquid equilibrium [11]. The triplet point among vapor, ordered CP1 solid and plastic solid is found to be at the reduced temperature of 0.282. The determination of the phase diagram involving solid phases was done by explicitly calculating the free energy (or chemical potential) with the Einstein-crystal method. In general, it is preferred to use the free energy calculation to determine phase equilibrium involving crystal phases. In fact, by conventional molecular simulations, it is difficult to observe phase transition between crystals consisting of slender molecules of large anisotropy.

In this work, we study the solid-solid phase transition of LJ dumbbell molecule between the ordered crystal of CP1 structure and the disordered crystal of FCC structure. We chose diatomic models of short bond lengths because these near-spherical molecules can rotate relatively easily in the crystal. As a benefit of the almost spherical molecular shapes, phase transformation between different crystal structures may actually occur in the course of molecular simulations. First, we performed *NPT* MC simulations to determine the crystal structure and the equilibrium positions and orientations of the molecules. In doing so, spontaneous order-disorder transitions are observed by varying the temperature and pressure. These spontaneous crystal-crystal transitions, although they are not in true thermodynamic equilibrium, may give a rough picture of phase changes, and it could serve as a criterion to check whether our free energy calculation is correct. Next, the free energies of the crystals are calculated by using the expanded ensemble Monte Carlo (EEMC) method and the thermodynamic integration (TI) method [4-6]. Coexistence condition for the solid-solid equilibrium is determined from the equality of chemical potential, and its consistency is checked by comparing with the transition behavior observed in the *NPT* MC simulations.

In calculating the free energy of ordered crystal consisting of symmetric molecules, a symmetric functional form that reflects the symmetry of the molecule may be used for the external rotational potential of the reference Einstein crystal [12]. Alternatively, asymmetric functional form may also be used if the crystal is *strongly* ordered without having orientational defect [13]. Since the details of the external potential function should not affect the free energy of real crystal, there must be a certain equivalence between the two different descriptions. We will investigate this aspect in great detail for the ordered crystals of LJ dumbbells with or without containing orientational defects, and we will also explain a criterion as to how we can choose a proper value of the symmetry number that depends on the form of external potential as well as the symmetry of the molecule by taking into account the rotational characteristics of the molecules in crystal.

THEORY AND SIMULATION METHOD

We study phase transitions between crystals made up of the LJ-d molecules of fixed bond length. Homonuclear diatomic molecules having near-spherical shapes with short reduced bond lengths of $L^*=0.225$, 0.250 and 0.275 are considered. These bond lengths are

chosen because the model molecules can rotate easily in crystal when phase transformation occurs between orientationally ordered and disordered crystals [8-10]. Two segments in different molecules interact by the Lennard-Jones interaction potential,

$$u(r)=4\varepsilon\left[\left(\frac{\sigma}{r}\right)^{12}-\left(\frac{\sigma}{r}\right)^{6}\right], \tag{1}$$

where u is potential energy, r is the distance between the two LJ segments, σ is the size parameter and ε is the well depth. As the LJ dumbbell is treated as a rigid body, bond vibration is not considered. In simulation, the intermolecular interaction is truncated at 3σ and standard long range corrections are considered. To determine crystal structure and the equilibrium positions and orientations of the molecules, we perform *NPT* MC simulations. The magnitudes of maximum translational and rotational moves of the molecules in MC simulation are chosen so as to yield about 50% acceptance. All nine degrees of the freedom of triclinic cell are fully explored to find the equilibrium crystal structure using the *NPT* MC algorithm of Yashonath and Rao [14]. Although not rigorous, the *NPT* MC simulation gives a rough sketch of phase transitions with hysteresis resulting from the metastability of condensed phase.

With a fixed crystal structure and density determined from the *NPT* MC simulation, the Helmholtz energy of crystal is calculated using the Einstein-molecule method [3]. In this method, an arbitrary chosen reference molecule, say, molecule 1 is fixed in space, and the translational degrees of freedom of the reference molecule are treated separately. This is contrasted with the conventional Einstein-crystal method [2] in which the center of mass of the system is constrained. To understand essential features of the Einstein-molecule approach, let us consider the partition function of a finite crystal consisting of N identical monatomic molecules as

$$Q=\frac{V}{N\Lambda^{3N}}\int\cdots\int\exp(-U/kT)d\mathbf{r}_2\cdots d\mathbf{r}_N, \tag{2}$$

where Q is the canonical partition function, U is the configurational energy, k is the Boltzmann constant, T is the temperature, V is the volume of system, Λ is thermal wavelength given by $\Lambda=h/(2\pi mkT)^{1/2}$ with h being the Planck constant and m being the mass of molecule, and $\mathbf{r}_i$ is the position vector of molecule i. In the Einstein-molecule approach, the reference molecule denoted by molecule 1 is fixed in space, while separately accounting for its contribution to the canonical partition function, V/Λ, the same as that of an ideal-gas molecule [3]. Also, by virtue of the fixed reference molecule the drift of crystal is avoided even when external potential is turned off when the system approach the real crystal.

The external potential for the reference Einstein crystal consisting of homonuclear diatomic molecules is given by

$$U^{Ein}(\mathbf{r},\theta)=\lambda_t\sum_{i=2}^{N}(\mathbf{r}_i-\mathbf{r}_{0,i})^2+\lambda_o\sum_{i=1}^{N}[1-\cos(n\theta_i)], \tag{3}$$

where λ_t is translational force constant, λ_o is rotational force constant, $\mathbf{r}_i$ is the position vector of the center of mass of molecule i, $\mathbf{r}_{0,i}$ is its equilibrium value, θ_i is angle made by the axis of molecule i and its equilibrium orientation and n is an integer that determines the periodicity of the external rotational potential. The equilibrium positions and orientations of the molecules are prepared from preliminary NVT MC simulation. The value of n may be chosen as n=1 for asymmetric potential or as n=2 for symmetric potential, respectively. The first term in the right-hand side of Eq. (3) is translational part of the external potential, and the last term represents rotational part for the molecule with line symmetry. The translational part for the Helmholtz energy of the reference Einstein crystal is given by [3,15]

$$\frac{\beta A_t^{Ein}}{N}=-\frac{1}{N}\ln\left(\frac{V}{N\Lambda^3}\right)-\frac{3}{2}\left(1-\frac{1}{N}\right)\ln\left(\frac{\pi}{\beta\lambda_t}\frac{1}{\Lambda^2}\right), \tag{4}$$

where A is the Helmholtz energy and β is 1/kT. The reduced form of Eq. (4) is written as

$$\frac{A_t^{Ein*}}{T^*}=-\frac{1}{N}\ln V^*-\frac{3}{2}\left(1-\frac{1}{N}\right)\ln\left(\frac{\pi}{\lambda_t^*}\right)-\frac{3}{2}\ln T^*, \tag{5}$$

where A^* is reduced Helmholtz energy per molecule (=A/Nε), T^* is reduced temperature (=kT/ε), and V^* is reduced volume (=V/Nσ^3), and λ_t^* is reduced force constant defined by $\lambda_t^*=\beta\lambda_t\sigma^2$. In deriving Eq. (5), we set, for convenience, the thermal wavelength Λ to $(T^*)^{-1/2}$ omitting factors independent of temperature. The values of the force constants of the external potential are chosen in a way such that each of positional and orientational distributions of the molecules in the Einstein crystal resembles the corresponding distribution in the real crystal. In fact, their precise values do not affect the free energy of the real crystal, but it is required that the configuration space of the reference system sufficiently overlap with that of the real system. For the present LJ-d crystal, the translational force constant is set to $\lambda_t^*=1000$ in the reduced unit. The rotational part for the free energy of the Einstein crystal is given by

$$\frac{\beta A_o^{Ein}}{N}=-\ln\left(\frac{8\pi^2 IkT}{\sigma_s h^2}\right)-\ln F_n(\beta\lambda_o), \tag{6}$$

where I is the moment of inertia of the molecule, σ_s is the symmetry number, and F_n is the excess contribution of the rotational part of the partition function due to the external rotational potential of the periodicity n. The reduced form of Eq. (6) is written as

$$\frac{A_o^{Ein*}}{T^*}=-\ln\left(\frac{T^*}{\sigma_s}\right)-\ln F_n(\lambda_o^*), \tag{7}$$

$$F_n(\lambda_o^*)=\begin{cases}\frac{1}{2}\int_0^{\pi}\exp[-\lambda_o^*(1-\cos\theta)]\sin\theta d\theta, & \text{for n=1 (asymmetric)}\\ \frac{1}{2}\int_0^{(\pi/2)\sigma_s}\exp[-\lambda_o^*(1-\cos 2\theta)]\sin\theta d\theta, & \text{for n=2 (symmetric)}\end{cases} \tag{8}$$

where λ_o^* is reduced rotational force constant (=$\beta\lambda_o$). The first terms in the right-hand sides of Eqs. (6) and (7) represent the ideal-gas contribution of rigid diatomic molecule. In deriving Eq. (7), we set, for convenience, $8\pi^2 I\varepsilon/h^2$ to unity. The integrals in Eq. (8) are evaluated numerically.

Whereas the symmetry number of a homonuclear diatomic molecule in gas and liquid phases is two, the symmetry number for the molecule confined in crystal depends on the extent of packing given by surrounding neighbor molecules. In orientationally disor-

dered crystal at high temperature, two indistinguishable orientational configurations are realized by the flipping rotation of molecule. Thus, the symmetry number is two so as not to overcount the identical configurations twice, which is the same reason as in the fluid phases. However, in orientationally ordered crystal at low temperature, the flipping rotation rarely occurs within finite observation time; only a single orientational configuration is realized out of the two possible configurations. The orientational distributions of the molecules, restricted by a high rotational barrier at $\theta=\pi/2$, are asymmetrically populated near the equilibrium orientation of $\theta=0$. Therefore, the proper value of symmetry number for the orientationally ordered crystal without rotational barrier-crossings (*strongly* ordered crystal) should be unity, $\sigma_s=1$. In the free energy calculation with $\sigma_s=1$, either asymmetric form (n=1) or symmetric form (n=2) for the external rotational potential of the ordered crystal may be used. When symmetric potential is used, the upper bound of the integral in Eq. (8) is $\pi/2$. This is because orientation angles beyond $\theta=\pi/2$ are never realized in the *strongly* ordered crystal at low temperature far below the order-disorder transition. A similar symmetric form of the external potential was used in the previous study of hard-dumbbell crystals [8]. In the discussion, we will demonstrate that there is a numerical equivalence between the symmetric and asymmetric external rotational potentials for calculating the free energy of the *strongly* ordered crystal.

Contrastingly, in orientationally ordered crystal at higher temperature close to the order-disorder transition there may occur rotational barrier-crossing or orientational defect. The onset of the rotational barrier-crossing does not usually coincide with the order-disorder transition, and it begins to occur at somewhat lower temperature than the transition temperature, while the orientations of the molecules in the crystal remain still ordered. This type of crystal is referred to as *weakly* ordered crystal. In terms of statistical mechanics, the rotational barrier-crossing gives rise to an abrupt expansion of the accessible region in the configuration space. Upon its occurrence, the configuration space of the real system might become quite different from that of the reference system, and the free-energy calculation with asymmetric external rotational potential would fail. To deal with the difficulty caused by the rotational barrier-crossing, the symmetric potential that reflects the molecular symmetry can be used instead [16]. For homonuclear diatomic molecule, the symmetric potential with $\sigma_s=2$ in Eq. (8) now covers the full range of the orientational angle, but by dividing the partition function by the symmetry number in Eqs. (6) and (7) overcounting flipped orientation by 180^o is avoided. Numerically, due to the symmetry of the potential, the value of the integral with $\sigma_s=2$ in Eq. (8) becomes twice than that with $\sigma_s=1$, but the free energy does not change due to the division by the symmetry number. Thus, the symmetric potential with $\sigma_s=2$ may also be used for the *strongly* ordered crystal, although the meaning of the symmetry number becomes less physical. The same prescription may be used for orientationally disordered (plastic) crystal, but since the orientational distribution in the disordered crystal is almost uniform, we do not need to use external rotational potential.

In addition, if the dumbbell molecule were regarded as a heteronuclear molecule consisting of two identical but distinguishable segments, the entropy per molecule would increase by k ln 2 for all phases. With regard to the *strongly* ordered crystal, since the diatomic molecule in crystal cannot make flipping rotation, the increase of entropy resulting from the segment-segment distinguishability is preserved as residual entropy, similarly as in the crystal of carbon monoxide. Therefore, the phase behaviors of molecular crystals have nothing to do with the distinguishability of segments or atoms because the entropy of each phase is changed by the same amount. In practice, the isotope effect on the phase behaviors is very small since the intermolecular interactions remain almost the same upon the exchange of isotopic elements.

In EEMC simulation of solid phase, the potential energy of the system varies linearly with a coupling parameter λ ranging from zero for the reference Einstein crystal to unity for the real crystal as

$$U(\lambda)=\lambda\sum_{i<j}u_{ij}+(1-\lambda)U^{Ein}, \tag{9}$$

The partition function of the expanded ensemble is a weighted sum of the partition functions of subensembles given by [17]

$$Q_E=\sum_i \exp(w_i)Q(N, V, T; \lambda_i), \tag{10}$$

Transition between adjacent subensembles ($\lambda_i \leftrightarrow \lambda_j$) is accepted by the Metropolis scheme with predetermined weight factor w_i. Free energy difference is derived from Eq. (10) as

$$\beta A_j-\beta A_i=w_j-w_i-\ln(P_j/P_i), \tag{11}$$

where P_i is the probability of observing the system with the coupling parameter λ_i during the EEMC simulation. The details of implementing the EEMC method for solid phase and optimizing the weight factors on the fly were described in our previous studies [18,19].

Once coexistence condition is determined at a fixed pressure, complete coexistence curve can be predicted by the Gibbs-Duhem integration method [20]. In fact, it is the same as integrating the Clapeyron equation given by

$$\frac{dP}{dT}=\frac{\Delta H}{T\Delta V}, \tag{12}$$

where ΔH and ΔV are differences in enthalpy and volume between two coexisting phases, respectively. Starting from a known transition temperature determined at zero pressure, we integrate Eq. (12) in discretized form while performing NPT MC simulations of the individual phases to obtain the enthalpy and volume.

RESULTS AND DISCUSSION

For crystals consisting of 500 LJ-d molecules of reduced bond lengths, 0.225, 0.25 and 0.275, *NPT* MC simulations were performed at various temperatures and pressures. Each simulation was done with an equilibration run of 2×10^5 cycles followed by a production run of 2×10^5 cycles. The simulation gives the equilibrium positions and orientations of the molecules as well as the crystal structure. Because of the small anisotropy of the molecule, ordered crystal at low temperature (at high pressure) readily transforms into orientationally disordered crystal as the temperature is raised (as the pressure is lowered), and phase transition between the two crystals is observed in the course of the *NPT* MC simulations.

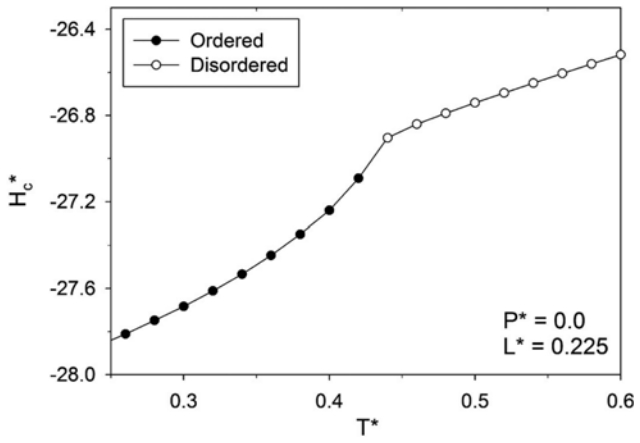

Fig. 1. The configurational enthalpy of the LJ-d crystal of L^*=0.225 at zero pressure.

Table 1. *NPT* MC simulation results for the configurational energy and the density of the LJ-d crystal of L^*=0.250 at zero pressure. The numbers in parentheses are simulation uncertainties in last digit

Ordered phase			Disordered phase		
T^*	U_c^*	ρ^*	T^*	U_c^*	ρ^*
0.30	−26.930(3)	0.9007(4)	0.456	−26.40(1)	0.8922(1)
0.32	−26.874(6)	0.8997(1)	0.458	−25.83(2)	0.8811(7)
0.34	−26.813(2)	0.8987(1)	0.46	−25.83(1)	0.8810(3)
0.36	−26.749(3)	0.8977(2)	0.48	−25.771(4)	0.87946(5)
0.38	−26.683(7)	0.8967(2)	0.50	−25.720(3)	0.8780(1)
0.40	−26.615(7)	0.89556(3)	0.52	−25.670(7)	0.8767(4)
0.42	−26.542(2)	0.89440(1)	0.54	−25.622(6)	0.8754(3)
0.44	−26.47(2)	0.8932(4)	0.56	−25.575(2)	0.87416(6)
0.46	−26.381(6)	0.8919(2)	0.58	−25.528(3)	0.8729(1)
0.48	−26.28(1)	0.8904(1)	0.60	−25.483(6)	0.8717(2)
0.49	−26.23(2)	0.8896(2)	0.62	−25.439(3)	0.87059(9)
0.492	−25.740(4)	0.8786(5)	0.64	−25.394(7)	0.8694(6)
			0.66	−25.349(4)	0.8683(2)

In Fig. 1, we show simulation results of the configurational enthalpy of the LJ-d crystal of L^*=0.225 at zero pressure. The configurational enthalpy is defined by $H_c=U_c+PV$, which becomes equal to the configurational energy U_c at zero pressure. The reduced configurational enthalpy per molecule, $H_c^*=H_c/N\varepsilon$, is plotted with respect to the reduced temperature. The LJ-d crystal at low temperature has orientationally ordered structure in which the rotational motions of the molecules are restricted. As the temperature increases, crystal structure becomes orientationally disordered FCC structure in which molecules rotate almost freely in the crystal. Two series of simulations were carried out along two opposite paths of increasing temperature (heating-up path) and of decreasing temperature (cooling-down path). The closed circles are simulation results obtained by following the heating-up path starting from an ordered crystal at low temperature, and the open circles are simulation results obtained by following the cooling-down path starting from a disordered crystal at high temperature, respectively. Both paths gave

Table 2. *NPT* MC simulation results for the configurational energy and the density of the LJ-d crystal of L^*=0.275 at zero pressure

Ordered phase			Disordered phase		
T^*	U_c^*	ρ^*	T^*	U_c^*	ρ^*
0.32	−26.146(2)	0.87911(7)	0.474	−25.652(1)	0.8700(1)
0.34	−26.087(2)	0.87807(7)	0.476	−24.831(8)	0.8530(3)
0.36	−26.0258(8)	0.87696(5)	0.48	−24.818(9)	0.8527(4)
0.38	−25.964(4)	0.8758(2)	0.50	−24.763(3)	0.8512(3)
0.40	−25.901(4)	0.87465(8)	0.52	−24.710(4)	0.8498(3)
0.42	−25.837(3)	0.87345(6)	0.54	−24.658(5)	0.8485(2)
0.44	−25.771(1)	0.8722(3)	0.56	−24.608(7)	0.8472(1)
0.46	−25.702(5)	0.87092(2)	0.58	−24.559(3)	0.8460(2)
0.48	−25.630(2)	0.8696(1)	0.60	−24.510(3)	0.8448(2)
0.50	−25.556(7)	0.8682(2)	0.62	−24.462(2)	0.8435(3)
0.52	−25.48(1)	0.8667(2)	0.64	−24.415(5)	0.8424(3)
0.54	−25.390(3)	0.8651(2)	0.66	−24.367(1)	0.84116(8)
0.56	−25.29(2)	0.8632(5)	0.68	−24.321(3)	0.83998(7)
0.574	−25.20(4)	0.8616(8)	0.70	−24.274(2)	0.8388(1)
0.576	−24.569(4)	0.8462(2)			

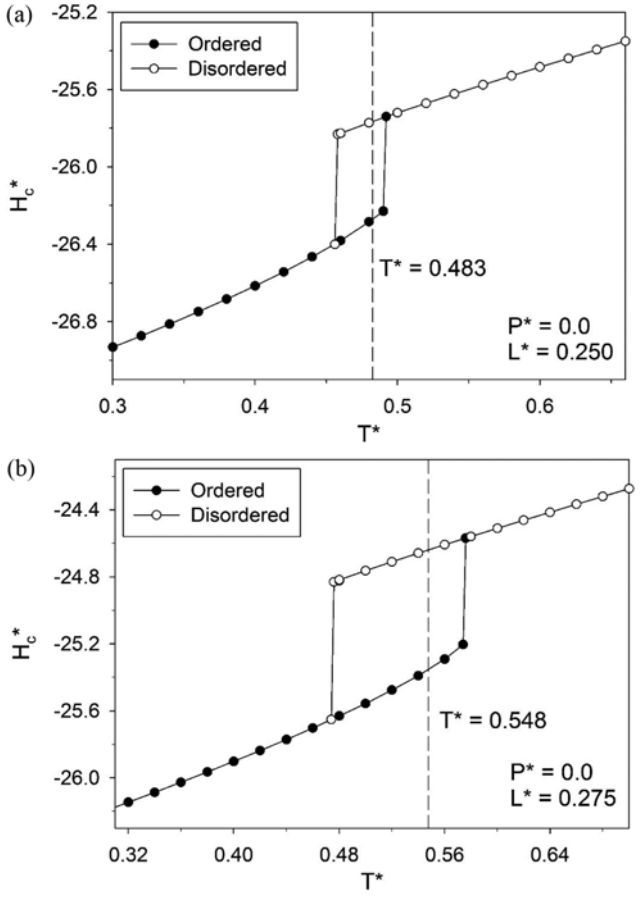

Fig. 2. The configuration enthalpy of the LJ-d crystals at zero pressure showing the first-order phase transition predicted by *NPT* MC simulation; (a) L^*=0.250 and (b) L^*=0.275. The vertical dashed line is the phase transition temperature predicted by the EEMC simulation (see Fig. 3).

the same results without showing hysteresis. Phase transition between the two crystal phases occurred at about T^*=0.44, but it appears to be the second-order phase transition, which is due to the small anisotropy of the molecule.

For the LJ-d models of larger anisotropies, L^*=0.250 and 0.275, the first-order phase transitions are clearly observed. In Tables 1 and 2 are given the NPT MC simulation results for the reduced configurational energy U_c^* ($=U_c/N\varepsilon$) and reduced density ρ^* ($=1/V^*$) of these crystals at zero pressure, and in Fig. 2 the reduced configurational enthalpies versus the reduced temperature are plotted. In each phase the density and configurational energy change gradually with the temperature, but they show discontinuous jumps between the two phases exhibiting the first-order phase transitions. The closed circles are for heating-up simulations starting from an ordered crystal of the CP1 structure, and the open circles are for cooling-down simulations starting from a disordered crystal of the FCC structure. Unlike the crystal of the smaller anisotropic molecule in Fig. 1, these crystals show hysteresis with different onsets of transitions along the opposite paths due to the metastability, which makes the condensed phase more or less resistant to phase transformation. The hysteresis loop becomes wider for the more slender molecule of L^*=0.275 than for the shorter one of L^*=0.250. This is because the molecules of longer bond can suppress the onset of transition more effectively with higher free-energy barrier. Unfortunately, the presence of hysteresis gives rise to a difficulty in finding equilibrium transition temperature (coexistence temperature). Thus, the *NPT* MC simulations can give at most rough estimates for lower and upper bounds of the transition temperature. These bounds might also depend on the finite size of the system. For the purpose of comparison, coexistence temperature determined by free-energy simulation is shown in Fig. 2 indicated by the vertical dashed line (the details will be explained with Fig. 3). The coexistence temperature is certainly within the hysteresis loop, but it is not simply at the middle of the hysteresis loop, somewhat shifted towards the upper bound of the transition temperature. At zero pressure, the coexistence temperature for L^*=0.250 is 0.483 in the reduced unit, and the coexistence temperature for L^*=0.275 is 0.548, respectively: The larger the bond length, the higher the coexistence temperature.

Using the EEMC simulation together with the Einstein-molecule approach, the Helmholtz energies of the LJ-d crystals were calculated, and the simulation results are presented in Table 3 for L^*=0.250 and Table 4 for L^*=0.275, respectively. The EEMC simulation was performed with the fixed crystal structure determined from the previous *NPT* MC simulation. The values in the third column of the table are the Helmholtz energies of the reference Einstein crystals A_{Ein}^* in the reduced unit, and values in the fourth column are differences in the Helmholtz energy between the Einstein crystal and the real crystal obtained from the EEMC simulation. In the last column, the values of the reduced Helmholtz energy of the real crystal A^* are given as the sum of the two contributions. The numbers in parentheses are simulation uncertainties in last digit estimated over five independent EEMC simulation runs. For the orientationally ordered crystal, symmetric external potential with the rotational force constant of λ_o^*=10 was used with the symmetry number of two. This somewhat small value of λ_o^* is used so that the flipping motion of molecule in the reference crystal occurs as frequently as in the real crystal at temperature close to transition. To obtain high precision results, the step size in coupling parameter was chosen as $\Delta\lambda$=0.01, and even finer step sizes were used for $\lambda\geq$0.90 to maintain the same order of precision and also to obtain flat distributions of subensembles along λ coordinate.

Table 3. The Helmholtz energy of the LJ-d crystal of L^*=0.250 at zero pressure obtained from the EEMC simulation. The numbers in parentheses are simulation uncertainties in last digit

T^*	Phase	A_{Ein}^*	ΔA^*	A^*
0.40	Ordered	6.109	−27.899	−21.789(4)
0.42	Ordered	6.363	−27.964	−21.600(4)
0.44	Ordered	6.615	−28.033	−21.418(2)
0.60	Disordered	6.358	−26.622	−20.264(2)
0.62	Disordered	6.519	−26.659	−20.139(9)
0.64	Disordered	6.679	−26.698	−20.019(5)
0.66	Disordered	6.837	−26.740	−19.903(3)

Table 4. The Helmholtz energy of the LJ-d crystal of L^*=0.275 at zero pressure obtained from the EEMC simulation

T^*	Phase	A_{Ein}^*	ΔA^*	A^*
0.42	Ordered	6.363	−27.107	−20.744(3)
0.44	Ordered	6.615	−27.169	−20.554(2)
0.46	Ordered	6.865	−27.235	−20.370(1)
0.64	Disordered	6.679	−25.721	−19.04(1)
0.66	Disordered	6.837	−25.763	−18.93(2)
0.68	Disordered	6.993	−25.810	−18.82(7)
0.70	Disordered	7.148	−25.848	−18.70(2)

In Fig. 3, the equilibrium transition temperatures of the LJ-d crystals of L^*=0.250 and 0.275 at zero pressure are predicted by the equality of the chemical potential (the molar Gibbs energy). To determine the transition temperature the Gibbs energies are calculated by the thermodynamic integration method as well as the EEMC method. The symbols are obtained from the EEMC simulations, and the curves are obtained from thermodynamic integration. For each phase, thermodynamic integration in temperature is carried out starting from a known value of free energy calculated by the EEMC simulation at a fixed temperature. To do this, we integrate the Gibbs-Helmholtz equation given by

$$\left[\frac{\partial(G/T)}{\partial T}\right]_p = -\frac{H}{T^2}, \tag{13}$$

where G is the Gibbs energy and H is the enthalpy of the system. The enthalpy is obtained by adding the average kinetic energy of linear rigid molecule, (5/2)RT, to the simulation value of the configurational enthalpy. The values of the enthalpy are then fitted with a polynomial of temperature, and the Gibbs-Helmholtz equation is integrated analytically. The results of the thermodynamic integrations are plotted as the curves in Fig. 3, and almost linear behaviors in temperature are observed. The values of the Gibbs en-

ergy obtained from both methods are in excellent agreement with each other, which confirms consistency and accuracy of the two free-energy calculations. By extrapolating the two curves in Fig. 3, the intersecting point gives the order-disorder transition temperature. The uncertainty of the transition temperature using different starting temperatures is estimated to be less than 1×10^{-3} in the reduced unit. From the comparison of Figs. 2 and 3, the phase transitions predicted by the NPT MC simulation and the EEMC simulation are in accord with each other.

In Table 5 are given the *NPT* MC simulation results for the configurational energy and density of the LJ-d crystals of L^*=0.275 at the reduced pressure of P^* ($=P\sigma^3/\varepsilon$)=10, and the configurational enthalpies varying with the temperature are plotted in Fig. 4. Note that there are significant contributions of *PV* term at high pressure. The transition occurs at higher temperature than that of the same system at zero pressure, which indicates that the increase of pressure enhances the stability of the ordered crystal. Also, the width of hysteresis loop becomes narrower in temperature. The vertical dashed line in Fig. 4 indicates equilibrium transition temperature of 0.687 obtained from the free-energy simulations (see Fig. 5). This

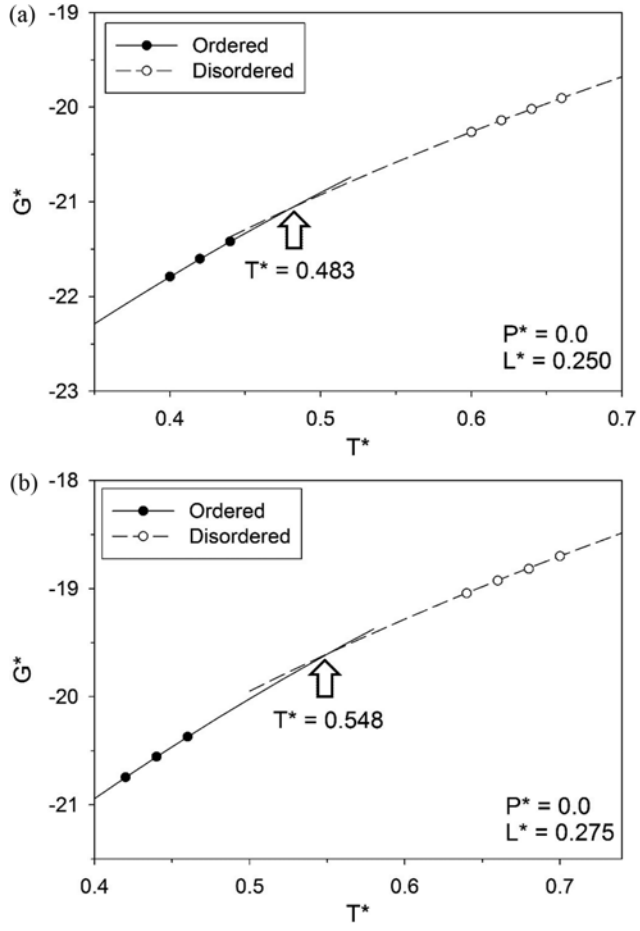

Fig. 3. The Gibbs energy of the LJ-d crystals at zero pressure obtained from MC simulations; (a) L^*=0.250 and (b) L^*=0.275. The symbols are from the EEMC simulations, and the curves are from the thermodynamic integration. The phase transition between orientationally ordered and disordered phases occurs at T^*=0.483 for (a) and at T^*=0.548 for (b), respectively. The simulation uncertainties are less than the size of the symbols.

Table 5. *NPT* MC simulation results for the configurational energy and the density of the LJ-d crystal of L^*=0.275 at P^*=10

Ordered phase			Disordered phase		
T^*	U_c^*	ρ^*	T^*	U_c^*	ρ^*
0.58	−25.439(8)	0.9047(1)	0.667	−25.13(3)	0.8998(4)
0.60	−25.376(5)	0.9036(3)	0.668	−24.53(2)	0.8916(5)
0.62	−25.308(3)	0.9026(1)	0.67	−24.525(7)	0.8915(1)
0.64	−25.24(1)	0.9015(2)	0.68	−24.502(9)	0.8909(2)
0.66	−25.16(3)	0.9003(4)	0.70	−24.46(1)	0.8899(6)
0.68	−25.06(3)	0.8989(4)	0.72	−24.421(4)	0.8889(2)
0.69	−25.00(7)	0.8981(6)	0.74	−24.383(5)	0.8879(2)
0.691	−24.99(9)	0.898(1)	0.76	−24.344(8)	0.8869(3)
0.692	−24.48(2)	0.8903(3)			

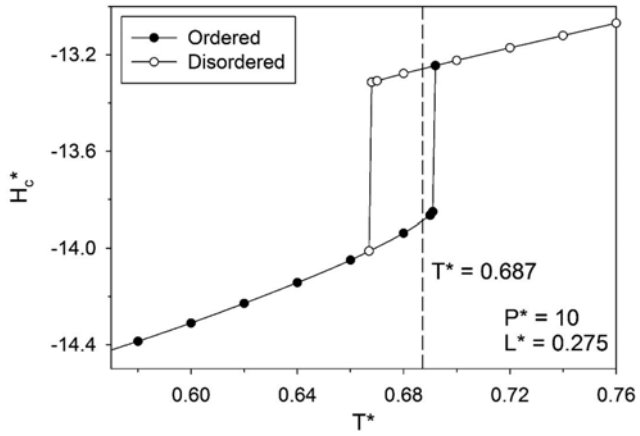

Fig. 4. The configuration enthalpy of the of LJ-d crystal of L^*=0.275 at P^*=10 obtained from NPT MC simulations. The meanings of the symbols and curves are the same as in Fig. 2.

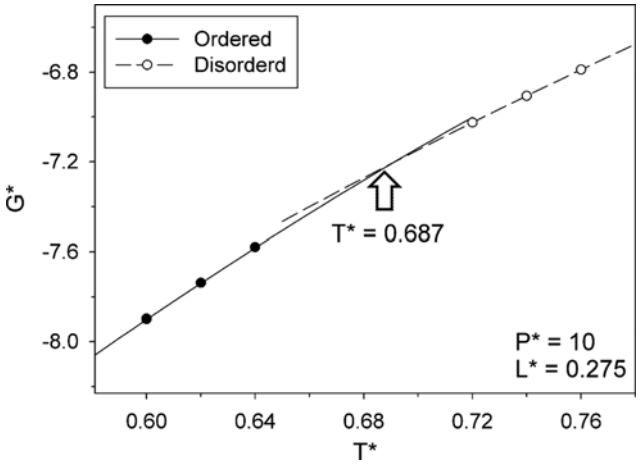

Fig. 5. The Gibbs energy of the LJ-d crystal of L^*=0.275 at P^*=10 obtained from MC simulations. The phase transition between the crystal phases occurs at T^*=0.687. The meanings of the symbols and curves are the same as in Fig. 3.

temperature is located within the hysteresis loop in accord with the phase behavior observed in the *NPT* MC simulations. However, the equilibrium transition temperature is a little shifted towards the disordered crystal phase in the hysteresis loop. This means that the disordered phase on transition would have to overcome higher free energy barrier than the ordered phase because aligning molecules to form an ordered structure would require extra free energy barrier.

In Table 6 are given the Helmholtz energies of the LJ-d crystals of L^*=0.275 at P^*=10 calculated by the EEMC simulation, and the corresponding Gibbs energies are plotted as the symbols in Fig. 5. Also, the Gibbs energies obtained from the thermodynamic integration method are plotted as the curves. Both of the free-energy simulation results are in excellent agreement with each other. The equality of the chemical potential is used to find the equilibrium transition temperature: By extrapolating the two isobaric curves intersecting point determines the order-disorder transition temperature, which is found to be 0.687 at P^*=10. Compared to the transition temperature of 0.548 at zero pressure as shown in Fig. 3(b), the transition temperature increases as the pressure increases.

In Tables 7 and 8 are presented the *NPT* MC simulation results for the configurational energy and density of the LJ-d crystals of L^*=0.275 at T^*=0.6 and 0.7, respectively. In these simulations, the pressure is varied at fixed temperature. Two opposite isothermal paths are simulated: pressure-raising path starting from a disordered crystal and pressure-reducing path starting from an ordered crystal. In Fig. 6 are shown the volumetric properties of the LJ-d crystals of L^*=0.275 at T^*=0.6 and 0.7. The closed circles are results for the pressure-reducing path, and the open circles are results for the pressure-raising path. Each of the paths shows a first-order transition with abrupt changes in the density and configurational energy,

Table 6. The Helmholtz energy of the LJ-d crystal of L^*=0.275 at P^*=10 obtained from the EEMC simulation

T^*	Phase	A_{Ein}^*	ΔA^*	A^*
0.60	Ordered	8.556	−27.522	−18.966(3)
0.62	Ordered	8.790	−27.607	−18.817(2)
0.64	Ordered	9.023	−27.695	−18.672(5)
0.72	Disordered	7.302	−25.577	−18.275(6)
0.74	Disordered	7.454	−25.622	−18.17(1)
0.76	Disordered	7.605	−25.669	−18.07(1)

Table 7. *NPT* MC simulation results for the configurational energy and the density of the LJ-d crystal of L^*=0.275 at T^*=0.6

Ordered phase			Disordered phase		
P^*	U_c^*	ρ^*	P^*	U_c^*	ρ^*
1.4	−24.573(6)	0.8529(2)	0.0	−24.51(1)	0.8448(5)
1.5	−25.16(5)	0.8672(7)	1.0	−24.557(7)	0.8506(3)
2.0	−25.21(6)	0.8701(7)	2.0	−24.595(8)	0.8563(4)
3.0	−25.26(2)	0.8751(4)	3.0	−24.625(6)	0.8618(1)
4.0	−25.308(7)	0.87982(5)	4.0	−24.649(8)	0.8671(4)
5.0	−25.34(1)	0.88423(9)	5.0	−24.67(1)	0.8722(5)
6.0	−25.36(1)	0.8884(1)	6.0	−24.68(1)	0.8772(3)
7.0	−25.37(2)	0.8924(3)	6.3	−24.683(1)	0.8787(2)
8.0	−25.379(6)	0.8963(3)	6.4	−25.36(1)	0.8900(2)
9.0	−25.379(6)	0.9000(1)			
10.0	−25.375(2)	0.9036(2)			

Table 8. *NPT* MC simulation results for the configurational energy and the density of the LJ-d crystal of L^*=0.275 at T^*=0.7

Ordered phase			Disordered phase		
P^*	U_c^*	ρ^*	P^*	U_c^*	ρ^*
11.0	−24.451(7)	0.8942(3)	6.0	−24.461(3)	0.87155(6)
11.2	−24.96(7)	0.9019(8)	7.0	−24.468(9)	0.8764(2)
12.0	−24.97(4)	0.9050(4)	8.0	−24.471(3)	0.8810(2)
13.0	−24.98(3)	0.9086(4)	9.0	−24.468(6)	0.8855(2)
14.0	−24.97(3)	0.9121(5)	10.0	−24.461(10)	0.8899(2)
15.0	−24.97(3)	0.9155(3)	11.0	−24.45(1)	0.8941(3)
16.0	−24.95(2)	0.9188(2)	12.0	−24.44(2)	0.8983(3)
17.0	−24.93(3)	0.9221(5)	13.0	−24.42(2)	0.9023(6)
18.0	−24.92(1)	0.9254(2)	13.5	−24.41(1)	0.9042(2)
			13.6	−24.98(2)	0.9108(4)

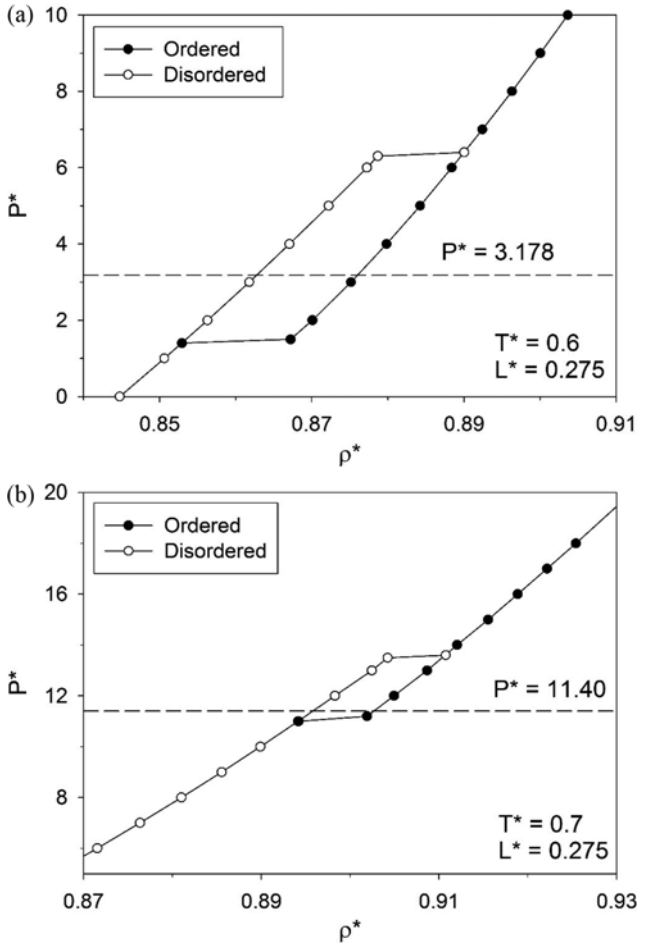

Fig. 6. The pressure-density curve of the LJ-d crystal of L^*=0.275; (a) T^*=0.6 and (b) T^*=0.7. The horizontal dashed line is the transition pressure predicted by the EEMC simulation (see Fig. 7).

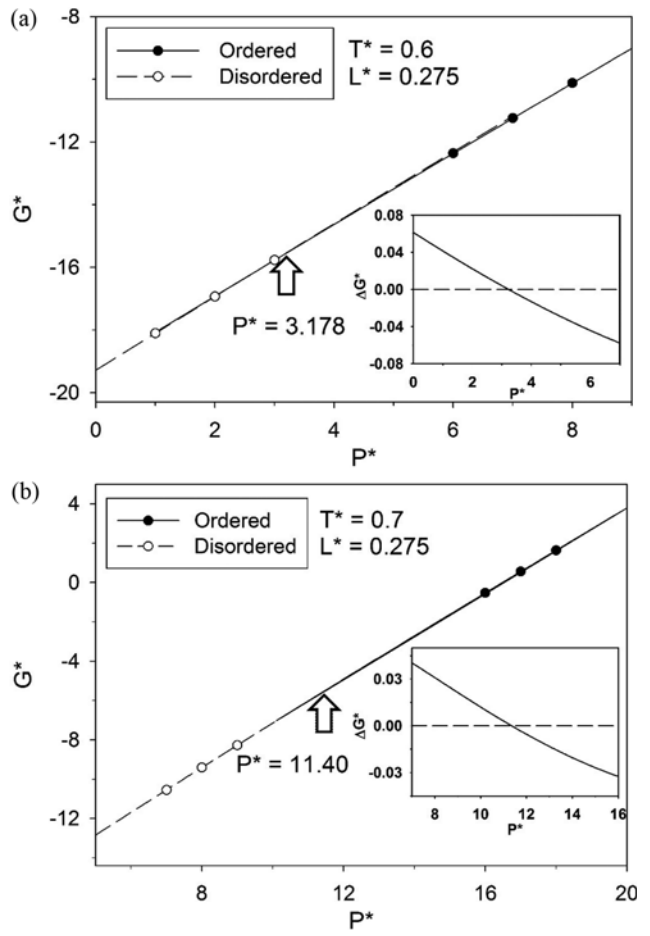

Fig. 7. The Gibbs energy of LJ-d crystal with L^*=0.275 obtained from MC simulation; (a) T^*=0.6 and (b) T^*=0.7. The symbols are from the EEMC simulations, and the curves are from the thermodynamic integration. Phase transition between the ordered and disordered phases occurs at P^*=3.178 for (a) and at P^*=11.40 for (b), respectively. The difference in the Gibbs energy between the two phases, $\Delta G^*=G^*$ (ordered)−G^* (disordered), is shown in the inset.

but they do not coincide with each other due to the hysteresis effects. Also shown are equilibrium transition pressures indicated by the horizontal dashed line determined from the free-energy simulations (see Fig. 7), of which the values are found to be P^*=3.178 for T^*=0.6 and P^*=11.40 for T^*=0.7, respectively. Disordered crystal beyond the equilibrium transition pressure and ordered crystal below the transition pressure are metastable phases. As the temperature increases, a transition occurs at higher pressure and density. Since the equilibrium transition pressure determined from the free-energy simulations is located within the hysteresis loop observed in the *NPT* MC simulation, both simulation results are consistent with each other. Specifically, the transition pressure tends to be in the lower region of the hysteresis loop. This means that on the spontaneous phase transition from disordered crystal to ordered crystal the system has to overcome higher free energy barrier than the reverse direction probably due to extra free energy barrier required for aligning the molecules to form ordered crystal structure.

In Tables 9 and 10 are given the Helmholtz energies obtained

Table 9. The Helmholtz energy of the LJ-d crystal of L^*=0.275 at T^*=0.6 obtained from the EEMC simulation

T^*	Phase	A_{Ein}^*	ΔA^*	A^*
1.0	Disordered	6.358	−25.637	−19.279(9)
2.0	Disordered	6.358	−25.625	−19.267(10)
3.0	Disordered	6.358	−25.606	−19.248(9)
6.0	Ordered	8.556	−27.672	−19.116(2)
7.0	Ordered	8.556	−27.638	−19.082(5)
8.0	Ordered	8.556	−27.602	−19.047(6)

Table 10. The Helmholtz energy of the LJ-d crystal of L^*=0.275 at T^*=0.7 obtained from the EEMC simulation

P^*	Phase	A_{Ein}^*	ΔA^*	A^*
7.0	Disordered	7.148	−25.679	−18.531(4)
8.0	Disordered	7.148	−25.634	−18.49(1)
9.0	Disordered	7.148	−25.584	−18.44(1)
16.0	Ordered	9.712	−27.653	−17.941(2)
17.0	Ordered	9.712	−27.590	−17.878(2)
18.0	Ordered	9.712	−27.523	−17.811(4)

from the EEMC simulation for the LJ-d crystals of L^*=0.275 at T^*= 0.6 and 0.7, respectively. Adding the *PV* term, we plot simulation results for the Gibbs energies of the crystals at T^*=0.6 in Fig. 7(a) and those at T^*=0.7 in Fig. 7(b), respectively. The equilibrium transition pressure between the two phases is determined by the equality of the chemical potential (the molar Gibbs energy). To calculate the transition pressure accurately, we performed thermodynamic integration of the following thermodynamic relationship:

$$\left(\frac{\partial G}{\partial P}\right)_T = V. \tag{14}$$

Fitting the simulation results of the volume with a polynomial of pressure, the integration of Eq. (14) is done analytically for each phase. This tells us how the Gibbs energy changes with the pressure, and the absolute value of the Gibbs energy is obtained by referring to a known value of the free energy which was calculated from the EEMC simulation. In Fig. 7, the results of the thermodynamic integrations are drawn as curves, and they are compared with the results of the EEMC simulations plotted as the symbols. Both results are in excellent agreement with each other. Extrapolating the two curves, the intersecting point determines order-disorder transition pressure, which is found to be P^*=3.178 at T^*=0.6 and P^*=11.40 at T^*=0.7, respectively. Note that the Gibbs energies of the two phases at the same pressure differ only slightly from each other, and the slopes of the two curves in Fig. 7 are at first glance almost the same. Thus, high-precision simulation results for the free energy are needed so as to determine the transition pressure accurately. For clarity, difference in the Gibbs energy, $\Delta G^*=G^*$ (ordered)−G^* (disordered), is shown in the inset of Fig. 7. Over the range of pressure we studied, the Gibbs energy difference between the two phases changes very slightly within 0.1 in the reduced unit whereas the Gibbs energy itself changes significantly with the pressure. Despite the small Gibbs energy differences, equilibrium order-disorder phase transition is

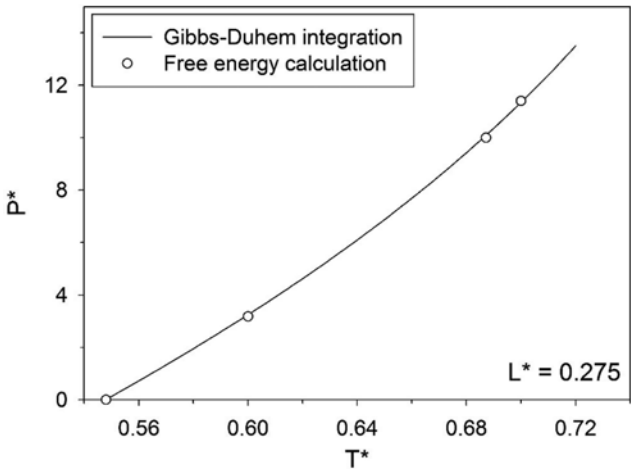

Fig. 8. The coexistence between the ordered and disordered LJ-d crystal of L^*=0.275. The symbols are obtained from the EEMC simulation and thermodynamic integration method, and the curve is obtained from the Gibbs-Duhem integration method.

well captured by the present free-energy calculations, and the predicted transition pressure is in accord with the transition behavior observed in the conventional *NPT* MC simulations as seen in Fig. 6.

Using the Gibbs-Duhem integration method [20], we predict a complete coexistence curve between the ordered and disordered LJ-d crystals of L^*=0.275. We integrate Eq. (12) using the Euler method with the step size of ΔT^*=0.0016 starting from a known coexistence condition of T^*=0.548 at zero pressure. The values of ΔH and ΔV are obtained from the *NPT* MC simulations of the individual phases. Each *NPT* MC simulation is carried out with an equilibration run of 2×10^4 cycles followed by a production run of 5×10^4 cycles. In Fig. 8, the coexistence curve obtained from the Gibbs-Duhem integration method is shown on the *PT* diagram. The upper left region is ordered crystal phase, and the lower right region is disordered crystal phase. The symbols are the coexistence conditions independently predicted by the previous free-energy calculations at P^*=0, P^*=10, T^*=0.6 and T^*=0.7. Except for the starting point at P^*=0, the coexistence curve obtained from the Gibbs-Duhem integration agrees well with the coexistence conditions obtained from the free-energy calculations with explicitly satisfying the equality of the chemical potential.

Throughout the free-energy calculations of the ordered LJ-d crystals, we have used the symmetric form for the external rotational potential with the symmetry number of two. This prescription works well for the ordered crystals with rotational barrier crossings (or rotational defects) that occur occasionally when the system is close to the order-disorder transition. This is a clear advantage of the symmetric external potential over the asymmetric one. When rotational barrier crossing does not occur at very low temperature (or at very high pressure), both potential forms are equally valid. In fact, the value of the free energy of real crystal ought not to depend on the details of the external potential used to represent the reference system. To elucidate this point, we calculated the Helmholtz energy of the ordered crystal at T^*=0.1 using both asymmetric and symmetric external rotational potentials, and compared the

Table 11. The comparison of the Helmholtz energies obtained by using asymmetric and symmetric external rotational potentials for the ordered LJ-d crystal with L^*=0.275 at T^*=0.1 and zero pressure

External potential	σ_s	λ_t^*	λ_o^*	A_{Ein}^*	ΔA^*	A^*
Asymmetric	1	1000	500	2.1291	−26.902	−24.773(1)
Symmetric	1	1000	250	2.1983	−26.972	−24.774(1)

results. Thermal energy at this low temperature is much less than the energy required to cross over the rotational barrier, and as a result, flipping rotation of the molecule does not occur during the simulation. Such *strongly* orientationally ordered crystal is a nonergodic system that physically accesses only a fragment of the whole orientational configuration space. In the free-energy calculation of the *strongly* orientationally ordered crystal, the symmetry number is set to unity for both forms of the external rotational potential.

To have the positional and orientational distributions of the reference crystal as close as those of the real crystal, we chose the translational force constant of the reference crystal to be λ_t^*=1000, and orientational force constants of asymmetric and symmetric potentials in Eq. (8) to be λ_o^*=500 and 250, respectively. In both cases, the orientations of the molecules stay close to the equilibrium orientation of θ=0. In the case of using symmetric potential, although there is another potential-energy minimum at flipped orientation $\theta=\pi$, it is never reached by physical process because molecules with low thermal energy can hardly jump over the high rotational barrier at $\theta=\pi/2$. As the forms of the external potential functions and potential parameters are different, the Helmholtz energies of the two reference Einstein crystals differ from each other as shown in Table 11. However, the final values of the Helmholtz energy of the real crystal calculated from the EEMC simulations are almost the same with negligible uncertainties in the fifth significant digit. This confirms well the methodological equivalence between the two methods of using the asymmetric and symmetric external rotational potentials.

Irrespective of which form of the external rotational potential is used, it is necessary to have the reference system access the phase space in a similar way as the real system. When flipping rotation is completely suppressed as in the *strongly* ordered crystal, the system accesses only a half of the orientational configuration space, and, correspondingly, the proper symmetry number for the reference crystal is unity. When flipping rotation occurs as in the *weakly* ordered crystal, the system now accesses the whole region of the orientational configuration space, and the proper symmetry number for the reference crystal should be two. The same statement applies to the disordered crystals.

Finally, we analyze the orientational distributions of the diatomic molecules in crystals. The distributions were obtained from the *NPT* MC simulations of the LJ-d crystals of L^*=0.275 at T^*=0.10 (*strongly* ordered crystal), at T^*=0.54 (*weakly* ordered crystal) and at T^*=0.56 (disordered crystal) all at zero pressure. In Fig. 9(a), we compare the orientational distributions of the two ordered crystals. The direction of θ=0 is set to coincide with the equilibrium orientation of the axis of the molecule. In the *strongly* ordered crystal at T^*=0.10, there is a single peak for the distribution of the axis

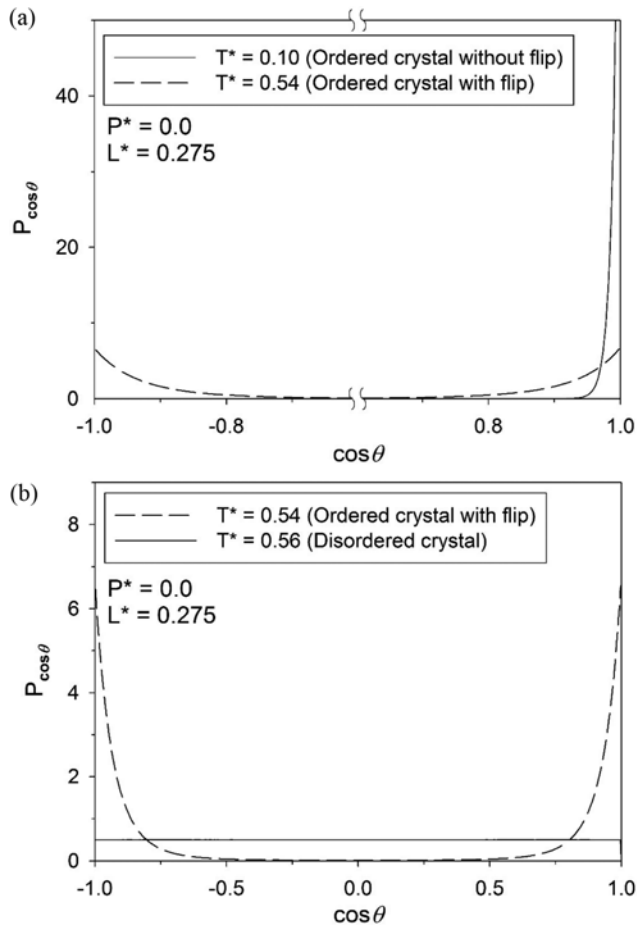

Fig. 9. Orientational probability distributions of the LJ dumbbells of L^*=0.275 in crystal phases; (a) the probability distributions at T^*=0.10 and T^*=0.54 both in the ordered crystals, and (b) the probability distributions at T^*=0.54 in the ordered crystal and at T^*=0.56 in the disordered crystal.

angles about the equilibrium orientation. This implies that the temperature is low enough that the flipping rotation of molecule is almost completely suppressed in the simulation. As seen in Table 11, this is the reason that the free energy calculation at sufficiently low temperature is possible with either asymmetric or symmetric external rotational potential with the symmetry number of unity. In contrast, in the *weakly* ordered crystal at T^*=0.54, there are two symmetric peaks in the orientational distribution. This indicates that enhanced thermal motion at higher temperature allows the flipping rotation of molecule to occur occasionally. As a result, the system now visits the whole orientational configuration space. If asymmetric external potential were used for this kind of *weakly* ordered crystal, the free energy calculation would fail because of the mismatch of the configuration spaces, which has been referred to as the rotational defect [4]. In Fig. 9(b), we compare the orientational distribution of the molecules in the ordered crystal at T^*=0.54 and that in the disordered crystal at T^*=0.56. Although the temperature difference is small, the structures of the two crystals and their orientational distributions are quite distinct. In contrast to the two symmetric peaks for the orientational distribution in the *weakly* ordered crystal at T^*=0.54, the orientational distribution in the disordered crystal at T^*=0.56 shows a uniform probability distribution, which indicates that the dumbbell molecule rotates almost freely within its lattice cell. Considering that the densities of the two crystals differ only by 2.1%, the changes of the rotational characteristics are drastic.

CONCLUSIONS

We studied the orientational order-disorder transition between crystals composed of LJ diatomic molecules of small anisotropy (reduced bond length) to firmly establish a theoretical framework to predict coexistence condition between orientationally ordered and disordered crystal phases. Since the conventional *NPT* MC simulation suffers from hysteresis in locating the phase equilibrium, we employed the EEMC simulation and thermodynamic integration method to explicitly calculate the chemical potentials of the individual crystal phases. Despite its inherent shortcomings, the *NPT* MC simulation can serve as a guiding tool to check the validity of the present method of calculating the free energy of crystals and also of finding the way to choose the symmetry number correctly.

We simulated three LJ-d models of small anisotropies of which the reduced bond lengths are 0.225, 0.250 and 0.275. These models are near-spherical so that spontaneous crystal-crystal phase transitions are observed in the *NPT* MC simulations. It was found that the ordered crystal of the CP1 structure at low temperature (or at high pressure) transforms into the disordered crystal of the FCC structure as the temperature increases (as the pressure decreases). The crystal composed of the LJ-d model of L^*=0.225 shows an order-disorder transition, but the transition appears to be in second order because the anisotropy of the molecule is too small. For the crystals with larger anisotropies of L^*=0.250 and 0.275, we observed the first-order phase transitions with hysteresis in the *NPT* MC simulations. For these systems, the Helmholtz energies of the crystals were calculated using the EEMC simulation, and the free energy profiles of the individual phases were obtained from the thermodynamic integration method. The true thermodynamic order-disorder phase transition or the coexistence condition was determined by the equality of the chemical potential. Such predicted transition temperature (or transition pressure) is found to be within the hysteresis loop of transition. This clearly indicates that the results of the present EEMC simulations are consistent with those of the *NPT* MC simulations.

To deal with the flipping rotations (rotational defects) of molecules in the ordered crystal close to order-disorder transition, we used a symmetric form for the external rotational potential with the symmetry number of two. Also, we demonstrated that when temperature is low enough that the ordered crystal is free of rotational defects, either symmetric or asymmetric form of the external rotational potential can be used with the symmetry number of unity. Finally, the Gibbs-Duhem integration was applied to the LJ-d crystal of L^*=0.275 in order to obtain a complete coexistence curve for the order-disorder phase transition. The coexistence curve is found to be in good agreement with the predictions from the free-energy calculations. This confirms again that the present simulation scheme to calculate the free energy of molecular crystal

agrees well with the conventional *NPT* MC simulation.

ACKNOWLEDGEMENT

This work was supported by the University of Seoul 2015 Research Fund.

NOMENCLATURE

A : Helmholtz energy
F : excess part of the partition function
G : Gibbs energy
H : enthalpy
H_c : configurational enthalpy
h : Planck constant
I : moment of inertia
k : Boltzmann constant
L : bond length
m : mass of molecule
N : number of molecules
n : periodicity of external rotational potential
P : pressure
P_i : probability of observing the i-th subsystem
Q : partition function
r : distance
r : position vector of molecule
$\mathbf{r}_0$: equilibrium position vector of molecule
T : temperature
U : total potential energy
U_c : configurational energy
u : intermolecular potential energy
V : volume
w : weight factor

Greek Letters

β : inverse of kT
ε : Lennard-Jones energy parameter
θ : axis angle
Λ : thermal de Broglie wavelength
λ : coupling parameter
λ_α : force constant
ρ : density
σ : Lennard-Jones size parameter
σ_s : symmetry number

Superscripts

Ein : Einstein crystal
* : reduced unit

Subscripts

E : expanded ensemble
o : orientation
t : translation

REFERENCES

1. D. Frenkel and A. J. C. Ladd, *J. Chem. Phys.*, **81**, 3188 (1984).
2. J. Polson, E. Trizac, S. Pronk and D. Frenkel, *J. Chem. Phys.*, **112**, 5339 (2000).
3. C. Vega and E. G. Noya, *J. Chem. Phys.*, **127**, 154113 (2007).
4. J. Chang and S. I. Sandler, *J. Chem. Phys.*, **125**, 054705 (2006).
5. M. Kim, J. Chang and S. I. Sandler, *J. Chem Phys.*, **140**, 084110 (2014).
6. M. Kim and J. Chang, *Korean J. Chem. Eng.*, **32**, 939 (2015).
7. S. J. Singer and R. Mumaugh, *J. Chem. Phys.,* **93**, 1278 (1990).
8. C. Vega, E. P. A. Paras and P. A. Monson, *J. Chem. Phys.,* **96**, 9060 (1992).
9. C. Vega, E. P. A. Paras and P. A. Monson, *J. Chem. Phys.*, **97**, 8543 (1992).
10. C. Vega and P. A. Monson, *J. Chem. Phys.*, **107**, 2696 (1997).
11. C. Vega, C. McBride, E. de Miguel, F. J. Blas and A. Galindo, *J. Chem. Phys.*, **118**, 10696 (2003).
12. J. W. Schroer and P. A. Monson, *J. Chem. Phys.*, **112**, 8950 (2000).
13. J. L. Aragones, E. G. Noya, C. Valeriani and C. Vega, *J. Chem. Phys.*, **139**, 034104 (2013).
14. S. Yashonath and C. N. R. Rao, *Mol. Phys.*, **54**, 245 (1985).
15. N. G. Almarza, *J. Chem. Phys.*, **126**, 211103 (2007).
16. C. Vega, E. Sanz, J. L. F. Abascal and E. G. Noya, *J. Phys.: Condens. Matter.*, **20**, 153101 (2008).
17. A. P. Lyubartsev, A. A. Martsinovski, S. V. Shevkunov and P. N. Vorontsov-Velyaminov, *J. Chem. Phys.*, **96**, 1776 (1992).
18. J. Chang and S. I. Sandler, *J. Chem. Phys.*, **118**, 8390 (2003).
19. J. Chang, *J. Chem. Phys.*, **131**, 074103 (2009).
20. D. A. Kofke, *J. Chem. Phys.*, **98**, 4149 (1993).